

Generation of parabolic laser pulses in short fibre amplifiers

I.A. Shchukarev, D.A. Korobko, M.Yu. Salganskii, I.O. Zolotovskii

Abstract. The laser pulse evolution in a normal-dispersion fibre amplifier is studied. The cases of ideal spectrum-homogeneous and transform-limited amplification are considered. It is shown that the envelope transformation of the input pulse to a parabolic form is possible not only for spectrally-flat amplification, but also for transform-limited one. In the latter case, an important parameter is the optimal amplifier length. The results demonstrate that, in the case of a sufficiently wide amplification spectrum, it is always possible to find the optimal amplifier length, after passing through which the output pulse envelope is close to a parabola.

Keywords: fibre amplifiers, parabolic pulses, normal dispersion.

1. Introduction

Pulsed fibre lasers and amplifiers are currently widely in demand in optical communications, materials processing, medicine, etc. [1, 2]. The need to further enhance the energy and peak power, as well as to reduce the duration of output pulses of fibre systems stimulates the development of new approaches to the amplification and generation of laser pulses. One of these approaches, intensively developing in recent decades, is the concept of similariton-like (self-similarly evolving) parabolic laser pulses with linear frequency modulation [3, 4]. Such pulses represent an ideal object for optical processing; in particular, they can be compressed with a high compression ratio both in temporal [5, 6] and spectral [7, 8] regions, with the attainment of a high peak power or spectral density.

Parabolic similariton pulses are an asymptotic solution of the nonlinear Schrödinger equation (NSE) with a constant gain in the case of normal dispersion [9]. This means that, in normal-dispersion fibre amplifiers, parabolic pulses, as one would think, should be formed automatically, acquiring high energy without critical distortions leading to the pulse destruction (wave-breaking effect [10]). However, unlike the ideal case described by the NSE, in real amplifiers the gain is not constant either in spectrum (due to the limited width of the gain line) or in length (due to the gain saturation). It has been shown that saturation does not limit the formation of parabolic similariton

pulses in the amplifier [11]; however, the limited spectral band of amplification is a critical factor. Indeed, the similariton spectrum width is proportional to $E^{1/3}$ (E is the pulse energy) [3], and when it grows up to the values comparable to the gain bandwidth, it is impossible to obtain a high-quality parabolic pulse of significant energy. A promising method for generating parabolic similaritons using passive fibres with normal dispersion decreasing in length [12] has not led as yet to breakthrough results. This is mainly due to the fact that the formation of a parabolic envelope requires the use of a fibre of considerable length, at which the negative effects of higher-order dispersions [mainly, third-order dispersions (TOD)] turn out critical [13]. Interesting results were obtained in the case of generation of parabolic pulses in long (~ 1 km) length-inhomogeneous Raman amplifiers [14]. Nevertheless, even in this case of small and sufficiently wide-band Raman amplification, the limitations caused by the spectral boundedness of the gain band and the presence of TOD did not allow one to obtain high-quality parabolic pulses with energies exceeding 1 nJ. The possibilities of generating parabolic pulses have been intensively studied in recent years. In this context we can mention, for example, papers [15, 16], in which the formation of parabolic pulses in long (hundreds of metres) length-inhomogeneous fibre amplifiers is considered by means of simulation, and attention is paid to the problem of TOD compensation. It is important to note that the amplification spectrum boundedness has not been taken into account in these works.

The object of this study is somewhat different from those above-specified – these are relatively short (not more than a few metres long) fibre amplifiers. Physically, they correspond to normal-dispersion Yb- or Er-doped fibres with sufficient high-power pumping. The aim of the work is a search for parameters of amplifiers providing the maximum closeness of the output pulse to a parabolic similariton.

2. Problem statement. Basic equations

Consider a fibre-optic amplifier with normal group velocity dispersion (GVD). The signal propagation in the amplifier is described by the Ginsburg–Landau equation for the complex field amplitude $A(z, t)$ [17]:

$$\frac{\partial A}{\partial z} - i \frac{\beta_2 - ig/\Omega_g^2}{2} \frac{\partial^2 A}{\partial t^2} + i\gamma |A|^2 A = gA, \quad (1)$$

where z is the longitudinal coordinate; t is the time in the travelling coordinate system; $\beta_2 > 0$ is the normal GVD coefficient; γ is the Kerr nonlinearity parameter of the fibre; and g is the gain. The dispersion dependence on the wavelength, i.e., higher dispersions (of the third and higher orders), is

I.A. Shchukarev, D.A. Korobko, I.O. Zolotovskii S.P. Kapitsa
Technological Research Institute, Ulyanovsk State University,
ul. L. Tolstogo 42, 432017 Ulyanovsk, Russia,
e-mail: blacxpress@gmail.com;

M.Yu. Salganskii G.G. Devyatikh Institute of Chemistry of
High-Purity Substances, Russian Academy of Sciences, ul. Tropinina
49, 603950 Nizhny Novgorod, Russia

Received 8 April 2019

Kvantovaya Elektronika 49 (10) 925–930 (2019)

Translated by M.A. Monastyrskiy

neglected, since the amplifier length is small. The contributions of higher nonlinearities (nonlinearity dispersions and SRS) are also not taken into account, since pulses with a duration of ~ 1 ps or more are considered, and again, because of small amplifier length. Equation (1) differs from the NSE by the presence of a term describing the spectrum-parabolic amplification, with the parameter Ω_g determining the gain line width (in s^{-1}), and also by the fact that, due to the saturation effect, the gain g depends on the amplifier length:

$$g = g_0 \left(1 + \frac{\int |A(z,t)|^2 dt}{E_{\text{sat}}} \right)^{-1}. \quad (2)$$

Here g_0 is the small-signal gain, and E_{sat} is the saturation energy. The parameters of the amplification system under consideration are as follows: $\gamma = 6 \text{ W}^{-1} \text{ km}^{-1}$, $\beta_2 = 50 \text{ ps}^2 \text{ km}^{-1}$, and $g_0 = 0.88 \text{ m}^{-1}$. As the initial pulse, a transform-limited Gaussian pulse with a duration of $\tau = 0.3 \text{ ps}$ and a peak power of $P = 100 \text{ W}$ is used. Next, we consider a few typical cases of the pulse evolution described by Eqn (1).

2.1. Spectrum-homogeneous amplification without saturation

This option corresponds to the NSE with a length-constant gain $g = g_0$, which can be obtained from (1) in the limiting case $E_{\text{sat}} \rightarrow \infty$, $\Omega_g \rightarrow \infty$. It is known that, under these conditions, the initial pulse with energy E_{in} (in this case $E_{\text{in}} \approx 75 \text{ pJ}$) and an arbitrary envelope transforms asymptotically (at $z \rightarrow \infty$) to the form of a parabolic similariton [3]:

$$A(z,t) = |A(z,t)| \exp(i\Phi(z,t)),$$

$$|A(z,t)| = A_0 \exp\left(\frac{2g}{3}z\right) \sqrt{1 - \frac{t^2}{t_p^2(z)}},$$

$$|t| < t_p, \quad |A(z,t)| = 0, \quad |t| > t_p, \quad (3)$$

$$t_p = \frac{3\sqrt{\gamma\beta_2/2}}{g} A_0 \exp\left(\frac{2g}{3}z\right), \quad A_0 = \frac{1}{2} \left(\frac{2gE_{\text{in}}}{\sqrt{\gamma\beta_2/2}} \right)^{1/3},$$

$$\Phi(z,t) = \varphi_0 + \frac{3\gamma A_0^2}{4g} \exp\left(\frac{4}{3}gz\right) - \frac{g}{3\beta_2} t^2.$$

Note that the asymptotic pulse chirp is determined by the gain and GVD: $\alpha = g/(3\beta_2)$; the similariton pulse duration t_p and, accordingly, the width $\Delta\Omega \approx 2\pi\alpha t_p$ of its spectrum increases exponentially with the length z .

Equation (1) with the specified parameters was simulated by the standard split-step Fourier transform method [17]. The simulation results in comparison with the asymptotic expressions are shown in Fig. 1. As can be seen, in the initial phase of amplification the pulse is far from asymptotics (3) (Fig. 1a). However, Eqn (3) describes, in fact, a nonlinear attractor of the dynamic system, which confirms the actual coincidence of the simulation results with the asymptotics after the pulse passes several metres in the amplifying fibre (Fig. 1b). As a characteristic of the difference between the $|A|^2$ value determined by the simulation of equation (1) and the analytical expressions for $|A|^2$ (3), we used the envelope misfit (MF) parameter ([14, 18]):

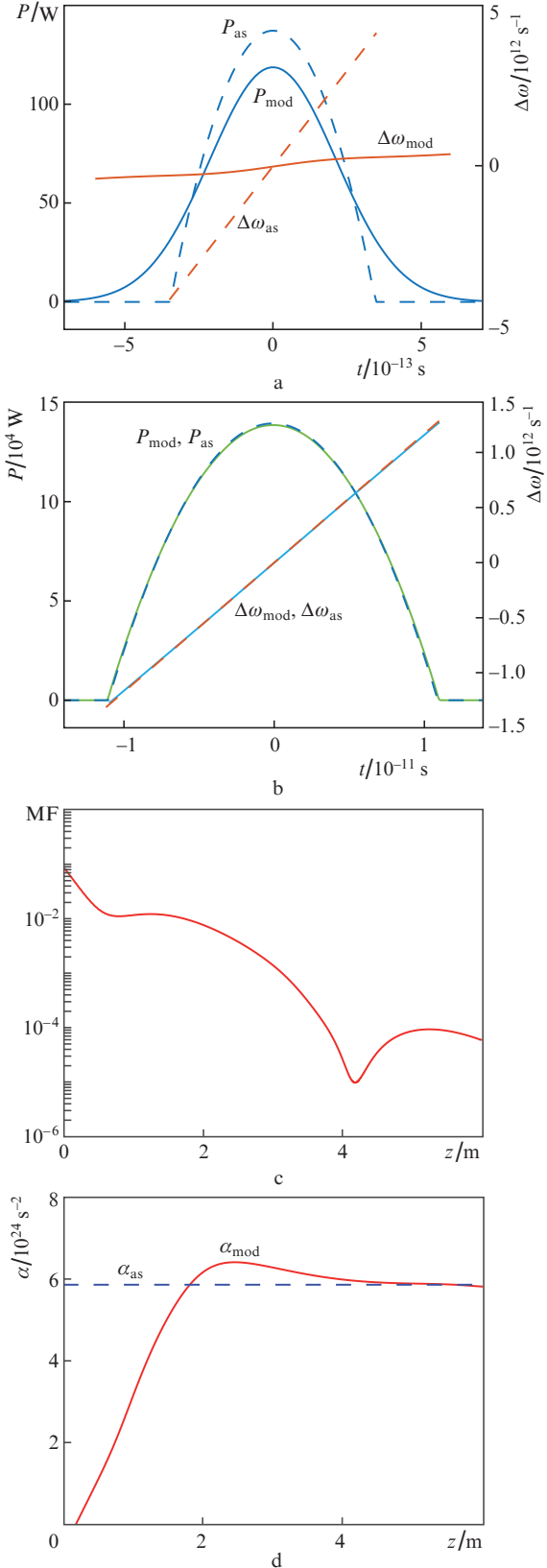


Figure 1. Spectrum-homogeneous amplification without saturation. The radiation pulse and the change in its instantaneous frequency at the amplifier length $L =$ (a) 0.1 and (b) 6 m. The results of simulation (solid curves) and calculation by asymptotic expressions (3) (dashed curves); (c) change in the envelope misfit parameter along the amplifier length; (d) chirp evolution, dashed line is the asymptotic limiting value $\alpha = g/(3\beta_2)$.

$$\text{MF} = \frac{\int [|\tilde{A}|^2 - |A|^2]^2 dt}{\int |\tilde{A}|^4 dt}. \quad (4)$$

Figures 1c and 1d additionally illustrate the above said: as the pulse amplifies, the envelope tends to a theoretically predicted parabolic form, and the chirp value approaches the asymptotic value $\alpha = g/(3\beta_2)$.

2.2. Spectrum-homogeneous amplification with saturation

This option can be obtained from (1) in the limit $\Omega_g \rightarrow \infty$ at a finite value of the saturation energy $E_{\text{sat}} < \infty$. To analytically solve the resulting equation, a variational method [19, 20] can be used, in which the probe pulse is written as a parabolic similariton pulse

$$u(z, t) = u_0(z) \sqrt{1 - \frac{t^2}{t_p^2(z)}} \exp[i\alpha(z)t^2 + \varphi(z)], \quad |t| < t_p. \quad (5)$$

The dynamic system equations for the time-averaged NSE Lagrangian,

$$\mathbf{L} = \frac{i}{2} \left(u \frac{\partial u^*}{\partial z} - u^* \frac{\partial u}{\partial z} \right) + \frac{\beta_2}{2} \left| \frac{\partial u}{\partial t} \right|^2 + \frac{\gamma}{2} |u|^4,$$

$$\frac{\partial \langle \mathbf{L} \rangle}{\partial \alpha} = 0, \quad \frac{\partial \langle \mathbf{L} \rangle}{\partial u_0} = 0, \quad \frac{\partial \langle \mathbf{L} \rangle}{\partial t_p} = 0,$$

lead to a system of equations describing the evolution of the pulse parameters during amplification:

$$\begin{aligned} \frac{du_0}{dz} &= g_0 u_0 \left(1 + \frac{4}{3} \frac{u_0^2 t_p}{E_{\text{sat}}} \right)^{-1} - \alpha \beta_2 u_0, \\ \frac{dt_p}{dz} &= 2\beta_2 \alpha t_p, \quad \frac{d\alpha}{dz} = -2\alpha^2 \beta_2 + \frac{u_0^2 \gamma}{t_p^2}. \end{aligned} \quad (6)$$

The saturation energy E_{sat} was chosen equal to 10 nJ (~ 135 energies of the initial pulse E_{in}). The initial values of the parameters of system (6) were chosen as follows: $u_0^2(0) = P = 100$ W, $\alpha(0) = 0$, $t_p(0) = \tau_p = 3\pi\tau/4 \approx 0.7$ ps, i. e., the energies and peak powers of the initial Gaussian pulse used for the simulation of Eqn (1) and those of the initial parabolic pulse evolving according to system (6) are equal. The results of simulating Eqn (1) are presented in Fig. 2 in comparison with the results of solving system (6). As in the previous case, we should emphasise the existence of a nonlinear attractor contributing to the formation of a parabolic envelope and linear frequency modulation. Naturally, with the same fibre length and saturable amplification, the pulse energy and its chirp magnitude turn out significantly smaller than those with constant amplification. It is important to point out the presence of a clear local minimum of the mismatch parameter (near $L \approx 3.8$ m) indicating the closeness of the pulse envelope to the parabola shape at a given point (Fig. 2c). However, at this time moment, frequency modulation rate (chirp) of the simulated pulse does

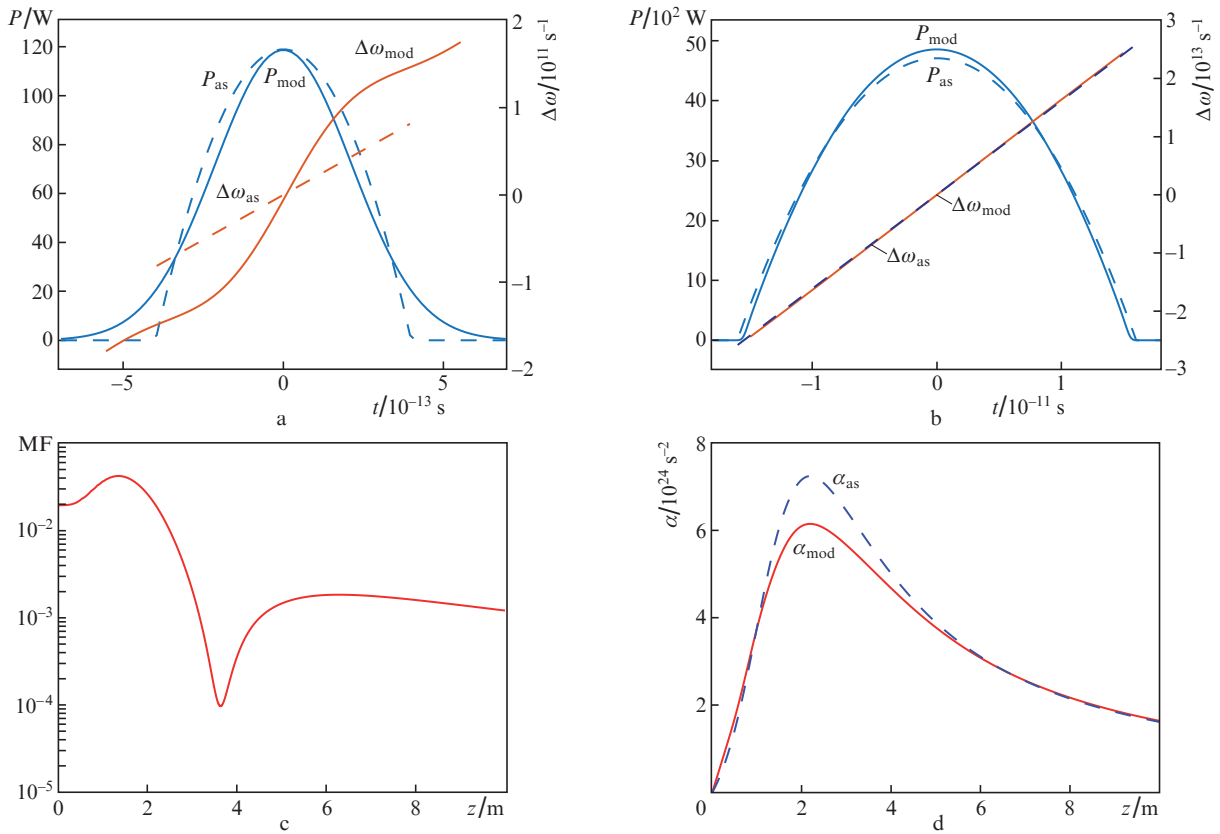


Figure 2. Spectrum-homogeneous amplification with saturation. The results of simulation (solid curves) and calculation by asymptotic expressions (3) (dashed curves). The radiation pulse and the change in its instantaneous frequency at the amplifier length $L =$ (a) 0.1 and (b) 10 m; (c) change in the MF parameter along the amplifier length; (d) evolution of frequency modulation rate (chirp).

not quite correspond to the value obtained from the variational calculations (Fig. 2d).

2.3. Transform-limited amplification with saturation

Next, consider the case that is closest to real fibre amplifiers, in which the gain line width is taken into account. To do this when simulating Eqn (1), the parameter Ω_g was chosen equal to 20 ps^{-1} , which corresponds to a gain bandwidth of $\sim 40 \text{ nm}$ in the wavelength range of ytterbium fibre lasers ($\lambda = 1050 \text{ nm}$). The saturation energy remains unchanged ($E_{\text{sat}} = 10 \text{ nJ}$).

The initial Gaussian pulse evolution in the fibre amplifier described by Eqn (1) is compared with the evolution of the parameters of the parabolic pulse described by system (6). A direct comparison of these processes is not entirely correct, because the Lagrangian L does not correspond to Eqn (1), which contains a transform-limited amplification term. Thus, other parameters being equal, the pulse evolving according to (1) receives less energy than the parabolic pulse whose parameters change according to (6). However, the research problem can be reformulated as follows: it is necessary to find the parameters of the fibre amplifier described by Eqn (1), which provide the maximum closeness of the amplified pulse envelope to a certain parabolic pulse that evolves in a system with uniform saturated amplification, i.e., the equality of initial energies is optional. (A pulse in the system with uniform amplification has a smaller initial energy.) As a result, the problem of finding the optimal parameters of a fibre amplifier, which are optimal for parabolisation, is reduced to finding the minimum of the envelope misfit functional (MF parameter value) similar to (4):

$$\text{MF} = \frac{\int [|A|^2 - |u|^2]^2 dt}{\int |A|^4 dt}. \quad (7)$$

In this case, optimisation at certain length L of a ‘real’ amplifier occurs not only at the expense of the choice of the parameters of Eqn (1), which determine the pulse $|A|^2$. By selecting the initial values of $t_p(0)$ and $u_0(0)$ in a certain range, we specify the parabolic pulse $u(z, t)$ of form (5), which evolves in the

amplifier with uniform saturable amplification and provides a minimum MF value.

Let us illustrate this by an example. The minimum value of functional (7) for the specified amplifier parameters is $\text{MF} \approx 9 \times 10^{-4}$ (the rightmost point in Fig. 3a). This value corresponds to $L = 2.03 \text{ m}$ at the initial parameters $u_0^2(0) = P$, $t_p(0) = 0.86\tau_p$ of the parabolic variational solution. Next, we calculate the minimum of this parameter with a decrease in the GVD of the amplifier. The results are presented in Fig. 3a. When searching for optimal values of the MF parameter, the amplifier length was varied in the range $1.5\text{--}2.5 \text{ m}$, while the values of $u_0(0)$ and $t_p(0)$ were varied in the range $(0.9\text{--}1)P$ and $(0.8\text{--}0.95)\tau_p$, respectively. As can be seen, at $\beta_2 = 30 \text{ ps}^2 \text{ km}^{-1}$ the minimum value of the envelope misfit parameter can be reduced to $\sim 5 \times 10^{-4}$. At this GVD value, having been optimised for the given amplification system ($\beta_2 = 30 \text{ ps}^2 \text{ km}^{-1}$), the dependence of the MF parameter minimum on the gain saturation energy E_{sat} is presented in Fig. 3b. The results show that the ‘parabolicity’ quality of the envelope at the optimal value $E_{\text{sat}} = 1 \text{ nJ}$ can be brought to a level that virtually corresponds to the ideal case of the spectrally homogeneous amplification with $\text{MF} \approx 3 \times 10^{-4}$. Naturally, however, that a drop in the output pulse energy becomes the payment for a decrease in the saturation energy.

Figure 4 shows the results characterising the initial pulse evolution under transform-limited amplification with the parameters $E_{\text{sat}} = 10 \text{ nJ}$ and $\beta_2 = 30 \text{ ps}^2 \text{ km}^{-1}$. When selecting the optimal amplifier length $L = 1.97 \text{ m}$, the output pulse envelope is close to a parabola (Fig. 4a). It is seen from Fig. 4b that the optimal length is determined quite clearly. If the amplifier length deviates from its optimum, the misfit parameter increases significantly. Despite the incomplete pulse chirp linearisation at a given length (we should note the nonlinear frequency modulation on the pulse wings) during the pulse passage through the linear dispersive element, there occurs a significant temporal compression of the pulse, accompanied by an increase in peak power. Figure 4c shows the envelopes of the output pulse and the output pulse passed through the linear dispersive element – a pair of diffraction gratings with anomalous dispersion $\beta_2 = -0.07 \text{ ps}^2 \text{ km}^{-1}$. A more than six-fold peak power increase indicates the linearity of frequency

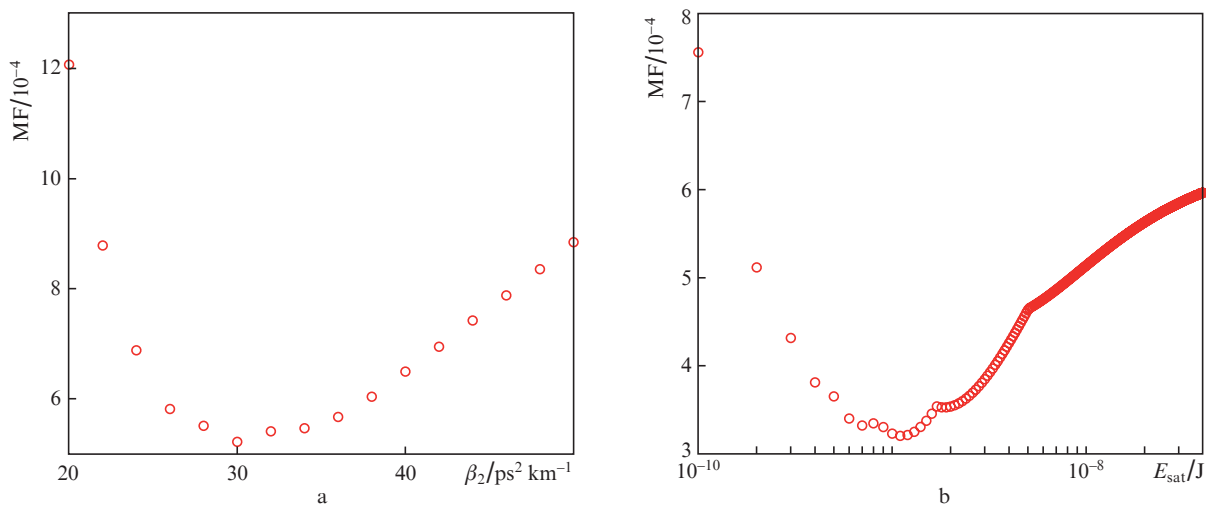


Figure 3. Minimum value of the MF parameter (7) at the transform-limited amplification with saturation as a function of (a) the amplifier GVD at $E_{\text{sat}} = 10 \text{ nJ}$ and (b) the amplifier saturation energy at $\beta_2 = 30 \text{ ps}^2 \text{ km}^{-1}$.

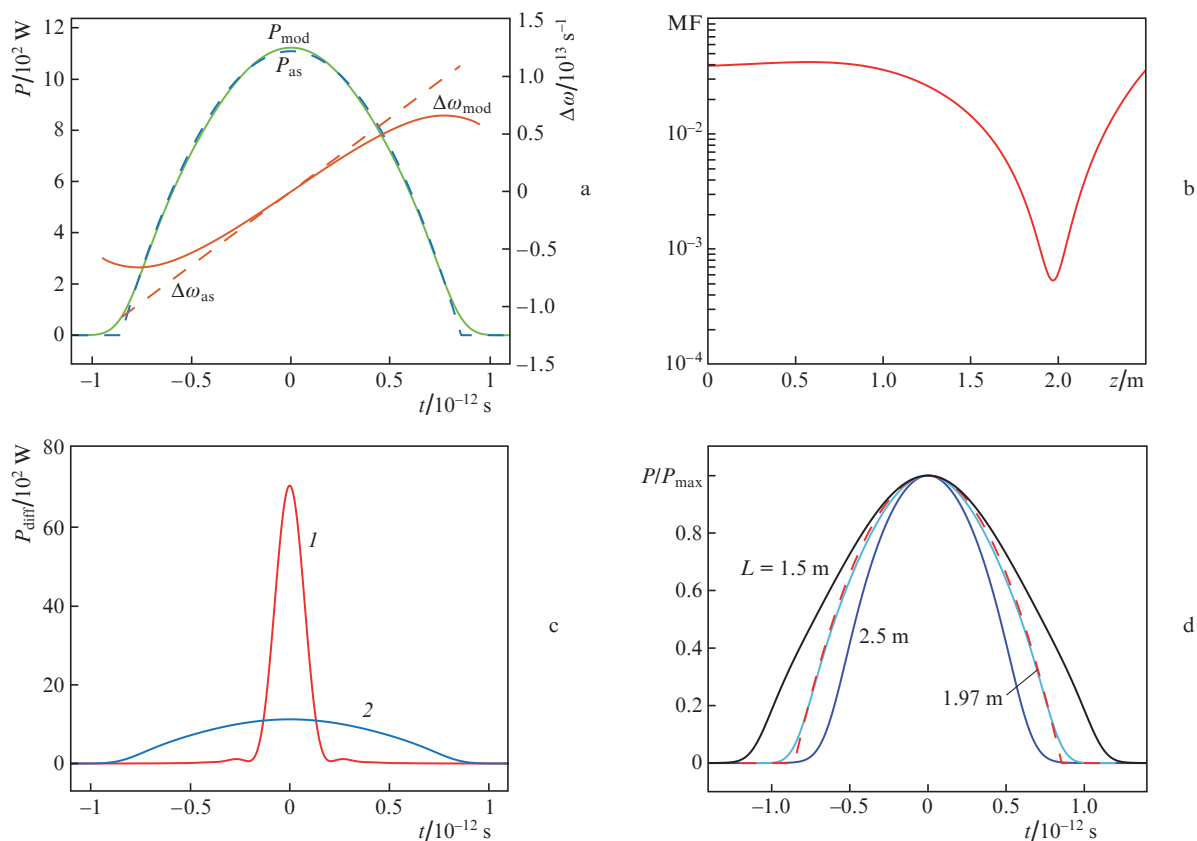


Figure 4. Transform-limited amplification with saturation; (a) radiation pulse and change in its instantaneous frequency at the amplifier length $L = 1.97$ m, the results of simulation (solid curves) and solution of the system (6) (dashed curves); (b) change of the MF parameter along the amplifier length; (c) pulse shape at the amplifier output at $L = 1.97$ m (1) and after compression at the output linear dispersion element (2); (d) normalised-to-maximum pulse envelope in the passage of amplifiers of various lengths, dashed curve shows the parabolic envelope.

modulation of the output pulse, sufficient for high-quality temporal compression. Figure 4d presents the envelopes of the output pulses passed through amplifiers of various lengths. One can see that, if the amplifier length is less than that optimal for parabolisation, the envelope retains a shape close to a Gaussian one. If the optimal length is exceeded, the pulse envelope becomes deformed and takes the triangle shape.

3. Discussion of the results. Conclusions.

The conducted studies of the laser pulse evolution in a nonlinear amplifier allow a number of conclusions to be drawn. The well-known fact of the existence in an amplification system with normal GVD and unlimited gain spectrum of a nonlinear attractor in the form of a parabolic similariton can be supplemented with an important observation. This asymptotic convergence is nonmonotonic and has a number of local minima (see Figs 1c and 2c) related to the gradual linearization of the pulse frequency modulation. When considering the transform-limited amplification, it can be noted that the first local minimum of the asymptotic convergence of the pulse to a parabolic form is also preserved in this case. In other words, with a wide enough gain spectrum, one can always find the optimal amplifier length, after passing through which the pulse will have an envelope close to a parabola (see Fig. 4). By optimising the GVD of the amplifier and pump, the differences in the envelope shape from a parabola can be minimised (Fig. 3). All these conclusions are made for short amplifiers, which justifies the neglect of the factors of highest dispersions (third-

order dispersions and higher) and nonlinearities (SRS and nonlinear dispersion) in our calculations. The proposed calculation method can be useful in setting up a series of experiments on the generation of pulses with parabolic envelope in real fibre amplifiers of optimal length. The developed generators of parabolic pulses can be used in systems for temporal and spectral compression [21, 22], optical processing [23], and also for subsequent amplification of pulses to ultrahigh energies [24, 25].

Acknowledgements. This work was supported by the Russian Science Foundation (Project No. 19-72-10037) and the Russian Foundation for Basic Research (Grant No. 18-42-732001).

References

1. Fermann M.E., Hartl I. *Nature Photon.*, **7**, 868 (2013).
2. Gumenyuk R., Okhotnikova E.O., Filippov V., Korobko D.A., Zolotovskii I.O., Guina M. *IEEE J. Sel. Top. Quantum Electron.*, **24**, 1 (2018).
3. Dudley J.M., Finot C., Richardson D.J., Millot G. *Nat. Phys.*, **3**, 597 (2007).
4. Ponomarenko S.A., Agrawal G.P. *JOSA B*, **25**, 983 (2008).
5. Tomlinson W.J., Stolen R.H., Shank C.V. *J. Opt. Soc. Am. B*, **1**, 139 (1984).
6. Fermann M.E., Kruglov V.I., Thomsen B.C., Dudley J.M., Harvey J.D. *Phys. Rev. Lett.*, **84**, 6010 (2000).
7. Andresen E.R., Dudley J.M., Oron D., Finot C., Rigneault H. *Opt. Lett.*, **36**, 707 (2011).
8. Korobko D.A., Okhotnikov O.G., Zolotovskii I.O. *JOSA B*, **33**, 239 (2016).

9. Kruglov V.I., Peacock A.C., Dudley J.M., Harvey J.D. *Opt. Lett.*, **25**, 1753 (2000).
10. Anderson D., Desaix M., Karlsson M., Lisak M., Quiroga-Teixeiro M.L. *J. Opt. Soc. Am. B*, **10**, 1185 (1993).
11. Bale B.G., Wabnitz S. *Opt. Lett.*, **35**, 2466 (2010).
12. Hirooka T., Nakazawa M. *Opt. Lett.*, **29**, 498 (2004).
13. Latkin A.I., Turitsyn S.K., Sysoliatin A.A. *Opt. Lett.*, **32**, 331 (2007).
14. Finot C., Barviau B., Millot G., Guryanov A., Sysoliatin A., Wabnitz S. *Opt. Express*, **15**, 15824 (2007).
15. Chowdhury D., Ghosh D., Basu M. *J. Opt.*, **20**, 095503 (2018).
16. Ghosh B.K., Ghosh D., Basu M. *J. Opt.*, **21**, 045503 (2019).
17. Agrawal G. *Nonlinear Fiber Optics* (New York: Springer, 2007).
18. Vukovic N., Broderick N.G.R., Poletti F. *Ad. Nonlin. Opt.*, **2008**, 1 (2008).
19. Zolotovskii I.O., Sementsov D.I., Senatorov A.K., Sysolyatin A.A., Yavtushenko M.S. *Quantum Electron.*, **40** (3), 229 (2010) [*Kvantovaya Elektron.*, **40** (3), 229 (2010)].
20. Zolotovskii I.O., Korobko D.A., Okhotnikov O.G., Sysolyatin A.A., Fotiadi A.A. *Quantum Electron.*, **42** (9), 828 (2012) [*Kvantovaya Elektron.*, **42** (9), 828 (2012)].
21. Finot C., Dudley J.M., Kibler B., Richardson D.J., Millot G. *IEEE J. Quantum Electron.*, **45**, 1482 (2009).
22. Abramov A.S., Zolotovskii I.O., Korobko D.A., Fotiadi A.A. *Opt. Spektrosk.*, **124** (3), 342 (2018).
23. Boscolo S., Finot C. *Intern. J. Opt.*, **2012**, 159057 (2012).
24. Korobko D.A., Okhotnikov O.G., Sysolyatin A.A., Yavtushenko M.S., Zolotovskii I.O. *J. Opt. Soc. Am. B*, **30**, 582 (2013).
25. Liu W., Schimpf D.N., Eidam T., Limpert J., Tünnermann A., Kärtner F.X., Chang G. *Opt. Lett.*, **40**, 151 (2015).